

Measurement of the η' -meson mass using $J/\psi \rightarrow \gamma\eta'$

J. Libby,¹ L. Martin,¹ A. Powell,¹ G. Wilkinson,¹ K. M. Ecklund,² W. Love,³
 V. Savinov,³ H. Mendez,⁴ J. Y. Ge,⁵ D. H. Miller,⁵ I. P. J. Shipsey,⁵ B. Xin,⁵
 G. S. Adams,⁶ M. Anderson,⁶ J. P. Cummings,⁶ I. Danko,⁶ D. Hu,⁶ B. Moziak,⁶
 J. Napolitano,⁶ Q. He,⁷ J. Insler,⁷ H. Muramatsu,⁷ C. S. Park,⁷ E. H. Thorndike,⁷
 F. Yang,⁷ M. Artuso,⁸ S. Blusk,⁸ S. Khalil,⁸ J. Li,⁸ R. Mountain,⁸ S. Nisar,⁸
 K. Randrianarivony,⁸ N. Sultana,⁸ T. Skwarnicki,⁸ S. Stone,⁸ J. C. Wang,⁸ L. M. Zhang,⁸
 G. Bonvicini,⁹ D. Cinabro,⁹ M. Dubrovin,⁹ A. Lincoln,⁹ P. Naik,¹⁰ J. Rademacker,¹⁰
 D. M. Asner,¹¹ K. W. Edwards,¹¹ J. Reed,¹¹ R. A. Briere,¹² T. Ferguson,¹²
 G. Tatishvili,¹² H. Vogel,¹² M. E. Watkins,¹² J. L. Rosner,¹³ J. P. Alexander,¹⁴
 D. G. Cassel,¹⁴ J. E. Duboscq,^{14,*} R. Ehrlich,¹⁴ L. Fields,¹⁴ R. S. Galik,¹⁴ L. Gibbons,¹⁴
 R. Gray,¹⁴ S. W. Gray,¹⁴ D. L. Hartill,¹⁴ B. K. Heltsley,¹⁴ D. Hertz,¹⁴ J. M. Hunt,¹⁴
 J. Kandaswamy,¹⁴ D. L. Kreinick,¹⁴ V. E. Kuznetsov,¹⁴ J. Ledoux,¹⁴ H. Mahlke-Krüger,¹⁴
 D. Mohapatra,¹⁴ P. U. E. Onyisi,¹⁴ J. R. Patterson,¹⁴ D. Peterson,¹⁴ D. Riley,¹⁴
 A. Ryd,¹⁴ A. J. Sadoff,¹⁴ X. Shi,¹⁴ S. Stroiney,¹⁴ W. M. Sun,¹⁴ T. Wilksen,¹⁴
 S. B. Athar,¹⁵ R. Patel,¹⁵ J. Yelton,¹⁵ P. Rubin,¹⁶ B. I. Eisenstein,¹⁷ I. Karliner,¹⁷
 S. Mehrabyan,¹⁷ N. Lowrey,¹⁷ M. Selen,¹⁷ E. J. White,¹⁷ J. Wiss,¹⁷ R. E. Mitchell,¹⁸
 M. R. Shepherd,¹⁸ D. Besson,¹⁹ T. K. Pedlar,²⁰ D. Cronin-Hennessy,²¹ K. Y. Gao,²¹
 J. Hietala,²¹ Y. Kubota,²¹ T. Klein,²¹ B. W. Lang,²¹ R. Poling,²¹ A. W. Scott,²¹
 P. Zweber,²¹ S. Dobbs,²² Z. Metreveli,²² K. K. Seth,²² and A. Tomaradze²²

(CLEO Collaboration)

¹*University of Oxford, Oxford OX1 3RH, UK*

²*State University of New York at Buffalo, Buffalo, New York 14260, USA*

³*University of Pittsburgh, Pittsburgh, Pennsylvania 15260, USA*

⁴*University of Puerto Rico, Mayaguez, Puerto Rico 00681*

⁵*Purdue University, West Lafayette, Indiana 47907, USA*

⁶*Rensselaer Polytechnic Institute, Troy, New York 12180, USA*

⁷*University of Rochester, Rochester, New York 14627, USA*

⁸*Syracuse University, Syracuse, New York 13244, USA*

⁹*Wayne State University, Detroit, Michigan 48202, USA*

¹⁰*University of Bristol, Bristol BS8 1TL, UK*

¹¹*Carleton University, Ottawa, Ontario, Canada K1S 5B6*

¹²*Carnegie Mellon University, Pittsburgh, Pennsylvania 15213, USA*

¹³*Enrico Fermi Institute, University of Chicago, Chicago, Illinois 60637, USA*

¹⁴*Cornell University, Ithaca, New York 14853, USA*

¹⁵*University of Florida, Gainesville, Florida 32611, USA*

¹⁶*George Mason University, Fairfax, Virginia 22030, USA*

¹⁷*University of Illinois, Urbana-Champaign, Illinois 61801, USA*

¹⁸*Indiana University, Bloomington, Indiana 47405, USA*

¹⁹*University of Kansas, Lawrence, Kansas 66045, USA*

²⁰*Luther College, Decorah, Iowa 52101, USA*

²¹*University of Minnesota, Minneapolis, Minnesota 55455, USA*

²²*Northwestern University, Evanston, Illinois 60208, USA*

(Dated: June 13, 2008)

Abstract

We measure the mass of the η' meson using $\psi(2S) \rightarrow \pi^+\pi^- J/\psi$, $J/\psi \rightarrow \gamma\eta'$ events acquired with the CLEO-c detector operating at the CESR e^+e^- collider. Using three decay modes, $\eta' \rightarrow \rho^0\gamma$, $\eta' \rightarrow \pi^+\pi^-\eta$ with $\eta \rightarrow \gamma\gamma$, and $\eta' \rightarrow \pi^+\pi^-\eta$ with $\eta \rightarrow \pi^+\pi^-\pi^0$, we find $M_{\eta'} = 957.793 \pm 0.054 \pm 0.036$ MeV, in which the uncertainties are statistical and systematic, respectively. This result is consistent with but substantially more precise than the current world average.

PACS numbers: 14.40.Cs, 14.40.Aq

*Deceased.

Experimental precision on the η' mass is currently worse than that of π , K , η , ω , or ϕ [1]. The PDG world-average value [1] is $M_{\eta'} = 957.66 \pm 0.24$ MeV. Recent experimental focus on the η mass has resolved a conflict among discrepant measurements [1]; the η' mass uncertainty now stands out in comparison to other narrow light mesons. This Letter presents a new measurement of the η' mass, the first in more than a decade.

The η and η' mesons are commonly understood as mixtures of the pure SU(3)-flavor octet ($u\bar{u} + d\bar{d}$) and singlet ($s\bar{s}$) states with possible admixtures of gluonium [2, 3]. The strengths of pseudoscalar and gluonium mixing become manifest in ratios of branching fractions for radiative decays of pseudoscalar (P) and vector (V) mesons, $V \rightarrow \gamma P$ and $P \rightarrow \gamma V$ [4, 5, 6]. However, these effects should also be evident in relationships between masses of η and η' on the one hand, and those of π and K mesons on the other. In the *current* (as opposed to *constituent*) quark framework, one such formulation for the pseudoscalar mixing angle in the flavor basis, ϕ_P , finds [7], to first order in flavor-symmetry breaking [8],

$$\tan^2 \phi_P = \frac{(M_{\eta'}^2 - 2M_K^2 + M_\pi^2)(M_\eta^2 - M_\pi^2)}{(2M_K^2 - M_\pi^2 - M_\eta^2)(M_{\eta'}^2 - M_\pi^2)}. \quad (1)$$

Using PDG [1] values for masses, $\phi_P = (41.460 \pm 0.009)^\circ$, which has an uncertainty dominated by ΔM_K ($\pm 0.007^\circ$), followed by $\Delta M_{\eta'}$ ($\pm 0.004^\circ$) and ΔM_η ($\pm 0.003^\circ$). This value for ϕ_P is consistent with determinations based upon branching fractions (which have uncertainties at the level of 1° [4, 5, 6]), indicating flavor-symmetry breaking effects are small [8]. In general, precision on most other predictions involving $M_{\eta'}$ has not yet matched that of experiment, and instead appears to be limited by theoretical assumptions and approximations [9, 10, 11]. More precise η' mass measurements will act as grounding for such predictions as they evolve.

This measurement is based upon data acquired with the CLEO detector at the CESR (Cornell Electron Storage Ring) symmetric e^+e^- collider, mostly in the CLEO-c configuration (95%) with the balance from CLEO III. The data sample corresponds to 27×10^6 [12] produced $\psi(2S)$ mesons, of which about 4×10^4 decay as $\psi(2S) \rightarrow \pi^+\pi^- J/\psi$, $J/\psi \rightarrow \gamma\eta'$. We employ three decay modes, denoted as A ($\eta' \rightarrow \rho^0\gamma$), B ($\eta' \rightarrow \pi^+\pi^-\eta$ with $\eta \rightarrow \gamma\gamma$), and C ($\eta' \rightarrow \pi^+\pi^-\eta$ with $\eta \rightarrow \pi^+\pi^-\pi^0$). The decay $J/\psi \rightarrow \gamma\eta$ with $\eta \rightarrow \pi^+\pi^-\pi^0$, denoted as mode D , is used to cross-check the analysis method. Other decay modes of η' and η were studied and found to have inadequate statistical precision compared to modes A - D . Because both $\psi(2S)$ and J/ψ are very narrow resonances with precisely known masses (J/ψ , ± 11 keV; $\psi(2S)$, ± 34 keV [1]), imposition of kinematic constraints enables a significant improvement in η' mass resolution. The analysis method and systematic error considerations are very similar to those of Ref. [13], in which $\psi(2S) \rightarrow \eta J/\psi$, $J/\psi \rightarrow \ell^+\ell^-$ decays were used to measure M_η .

The CLEO-c detector is described in detail elsewhere [14]; it offers 93% solid angle coverage of precision charged particle tracking and an electromagnetic calorimeter comprised of CsI(Tl) crystals. The tracking system enables momentum measurements for particles with momentum transverse to the beam exceeding 50 MeV/ c and achieves resolution $\sigma_p/p \simeq 0.6\%$ at $p=1$ GeV/ c . The barrel calorimeter reliably measures photon showers down to $E_\gamma=30$ MeV and has a resolution of $\sigma_E/E \simeq 5\%$ at 100 MeV and 2.2% at 1 GeV.

Signal and background processes are modeled with Monte Carlo (MC) samples that were generated using the EVTGEN event generator [15], fed through a GEANT-based [16] detector simulation, and subjected to event selection criteria. The distribution of “transition dipion” (the $\pi^+\pi^-$ emitted in the $\psi(2S)$ -to- J/ψ -transition) mass is sculpted [12] to match that of the data, and angular distributions of the J/ψ decay products are set to be appropriate for

a vector decay into a vector and a pseudoscalar. The decay $\eta \rightarrow \pi^+\pi^-\pi^0$ is generated using the matrix element measured in Ref. [17].

Event selection requires the tracking system to find exactly two oppositely-charged particles for the transition dipion, and two (A , B , and D) or four (C) more tracks of net charge zero. A minimum of two (A) or three (B , C , and D) photon candidates must also be found. Photons must be located in the central portion of the barrel calorimeter where the amount of material traversed is smallest and therefore energy resolution is best ($|\cos\theta_\gamma| < 0.75$, where θ is the polar angle with respect to the initial e^+ direction). Such photons must also have energy exceeding 120 MeV (A) or 36 MeV (B , C , and D), and either be more than 30 cm from any shower associated with one of the charged pions, or, when between 15 and 30 cm from such a shower, have a photon-like lateral shower profile. Selected photons cannot lie near the projection of any charged pion's trajectory into the calorimeter, or align with the initial momentum of any π^\pm candidate within 100 mrad. Spurious showers faking photons can result from nuclear interactions of charged pions in the calorimeter. Such showers tend to have low energy for which the MC modeling may be less accurate. Therefore we consider only the two (A) or three (B , C , and D) highest energy photon candidates satisfying the above criteria to suppress such mismodeling effects. Photon pairs are candidates for a π^0 or η if their invariant mass satisfies $M(\gamma\gamma) = 115\text{-}150$ MeV or $500\text{-}580$ MeV, respectively, and are then constrained to the PDG average π^0 or η masses [1].

Further kinematic requirements are applied in two two-step fits: first, the J/ψ decay products are constrained to originate from a single point (vertex) consistent with the beam spot and then constrained to have the J/ψ mass, $M_{J/\psi}$ [1]; quality restrictions are applied to both the vertex and the mass kinematic fits ($\chi^2/\text{d.o.f.} < 8$ for each). Second, the J/ψ candidate and transition dipion are constrained to a common vertex and then to the $\psi(2S)$ mass, $M_{\psi(2S)}$ [1], and three-momentum, including the effect of the $\simeq 3$ mrad crossing angle of the e^+ and e^- beams. Again, quality restrictions are applied to both the vertex and four-momentum kinematic fits ($\chi^2/\text{d.o.f.} < 8$ for each). The $\chi^2/\text{d.o.f.}$ distributions are shown in Fig. 1.

No attempt is made to isolate the $\eta \rightarrow \pi^+\pi^-\pi^0$ decay in mode C because this is difficult to achieve in an unambiguous way; frequently multiple such combinations per event are consistent with an η decay due to confusion between the dipion from the $\eta' - \eta$ transition and the dipion from the η decay. Therefore we do not take advantage of constraining any three-pion mass to that of the η as we do with $\eta \rightarrow \gamma\gamma$ in mode B . The η' mass is instead formed from the five pion four-momenta.

With these selections, the three samples of η' decays are very pure. Non- J/ψ decays are estimated to constitute up to a 0.5-1.0% background for all three η' modes, as determined by examining the recoil mass sidebands of the $\psi(2S)$ transition dipion for non- J/ψ contamination when the J/ψ vertex and mass fits are removed. Inspection of the ρ^0 , π^0 , η , and η' mass distributions, shown in Fig. 2, verify that J/ψ backgrounds are small. MC studies of J/ψ decays that might be expected to contaminate mode A , such as $J/\psi \rightarrow \rho^0\eta$ and $J/\psi \rightarrow \pi^+\pi^-\pi^0$ and cross-feed from $J/\psi \rightarrow \gamma\eta'$, $\eta' \rightarrow \pi^+\pi^-\eta$, $\eta \rightarrow \gamma\gamma$, are found to contribute only at the 0.1% level. These backgrounds show no significant structure or strong slope in the η' mass distributions, so their effects upon the mass determination are small compared with statistical uncertainties and are therefore neglected.

Each event yields an invariant mass M of the kinematically-constrained decay products; a single mass value is extracted for each decay mode i by fitting a Gaussian shape to the distribution of $\delta_i \equiv M_i - M_0$, where M_0 is a reference value, either the PDG2006 world-average

$M_{\eta'}^0 = 957.78$ MeV [18] (for historical reasons; the PDG2008 value is 957.66 ± 0.24 MeV [1]), or, in the case of mode D , the PDG2008 η mass central value. We define the symbols $\langle\delta\rangle$ and σ as the resulting Gaussian mean and width, respectively. The fits are restricted to the central portion of each δ distribution because the tails outside this region are not represented well by a single Gaussian form. The fits span $\pm 1.7\sigma$ to $\pm 2.1\sigma$ about $\langle\delta\rangle$, and in all cases the resulting fit has a confidence level exceeding 40%. The distributions of δ_i with overlaid fits are shown in Fig. 3. Other shapes that might fit the tails, such as a double Gaussian, have been found to yield unstable fits and/or do not improve precision of finding the peak.

There is an unavoidable low-side tail in any monochromatic photon energy distribution from the CLEO calorimeter. It originates from losses sustained in interactions prior to impinging upon the calorimeter and from leakage outside those crystals used in the shower reconstruction. This asymmetric photon energy resolution function causes a small but significant systematic bias in $\langle\delta\rangle$: for simplicity of the kinematic fitting formalism, input uncertainties are assumed to be symmetric, and a bias occurs if they are not. This bias in fitted Gaussian mean is mode-dependent because each presents a different mix of charged and neutral particles.

The biases β_i are estimated by following the above-described procedure on MC signal samples. Each β_i is the difference between the Gaussian peak value of the $M_{\eta'}$ distribution and the input $M_{\eta'}^{\text{MC}}$. We define the bias as $\beta_i \equiv \langle\delta_i\rangle_{\text{MC}}$, in which we use the MC input $M_{\eta'}^{\text{MC}}$ for M_0 . A non-zero value of β_i means that, for mode i , the Gaussian peak mass $\langle\delta_i\rangle$ is offset from the true mass and must be corrected. Although the asymmetric photon lineshape is responsible for most of this difference, the resulting correction automatically compensates for all modeled sources of bias. A bias value for the η cross-check is determined similarly.

Table I summarizes results by decay mode. The η mass result from mode D ($\langle\delta\rangle - \beta = 38 \pm 148$ keV) is consistent with expectations within its statistical uncertainty. The number of events involved in the determination of $M_{\eta'}$ in modes A , B , and C is 3917. The three values of $\langle\delta_i\rangle - \beta_i$ have an average, weighted by statistical errors only, of $(\langle\delta\rangle - \beta)_s = 15 \pm 53$ keV with a $\chi^2 = 0.14$ for two degrees of freedom, demonstrating consistency.

Systematic and statistical errors are summarized in Table II. Uncertainties that are uncorrelated mode-to-mode, including statistical, are used to determine the weights ($w_i = 0.44$, 0.47 , and 0.09 for A , B , and C , respectively) applied to combine values from the three modes into the weighted sum $(\langle\delta\rangle - \beta)_w = \sum_{i=1}^3 w_i \times (\langle\delta_i\rangle - \beta_i) = 13 \pm 54 \pm 36$ keV, where the uncertainties are statistical and systematic, respectively. Note that the combined value using weights including systematic errors is virtually identical to that obtained accounting only for statistical uncertainties.

As the mass distributions are not perfectly Gaussian, there is some systematic variation of the peak value with the choice of mass window for each fit. We vary the low- and high-side mass limits by ± 1 MeV, symmetrically, and note the variations in MC peak values with respect to the nominal mass window, as summarized in Table II.

Uncertainties attributable to imprecision in the masses of the J/ψ (11 keV), $\psi(2S)$ (34 keV), and η (24 keV) mesons [1] are directly calculated by repeating the analysis using an altered mass and the deviation in $\langle\delta\rangle$ per “ 1σ ” change from nominal taken as the error. Based on the studies in Ref. [13] we take one third of the bias magnitude plus its statistical uncertainty, $(|\beta_i| + \Delta\beta_i)/3$, as our estimate of the systematic uncertainty in bias, and here also add one third of its uncertainty due to MC statistics. Uncertainties in charged particle momentum and calorimeter energy scale are evaluated by shifting those scales by the appropriate amount and repeating the analysis. We quote a relative momentum scale accuracy

of 0.01% [13] and a calorimeter energy scale uncertainty of 0.6% [13] and use these values for our 1σ systematic variations. Any deviation from ideal in momentum or energy scale is substantially damped by the four-momentum constraints, as is evident from Table II: the momentum or energy scale 1σ uncertainties induce, at most, ≈ 3 parts in 10^5 shift in η' -mass scale.

To investigate the effect of less-well-measured events, we have repeated the analysis after tightening the kinematic fitting restrictions on each of the four kinematic fits per event from $\chi^2/\text{d.o.f.} < 8$ to < 3 , losing about half of the original events. The overall statistically-weighted η' mass changes by 0 ± 47 keV, in which the uncertainty is statistical, demonstrating stability of the measured mass with respect to the kinematic fit quality.

After combining the $(\langle \delta_i \rangle - \beta_i)$ values in Table I using the quoted weights and adding the $M_{\eta'}^0$ offset from above, our result is $M_{\eta'} = 957.793 \pm 0.054 \pm 0.036$ MeV, where the first error is statistical and the second is systematic. This result betters the precision of the world average by nearly a factor of four and has a central value consistent with it. The next most precise single measurement has a factor of five larger uncertainty [19] and is more than thirty years old. Three η' decay modes contribute to this result and are consistent with one another. This measurement brings the mass uncertainty to a level more comparable to that of K^0 or η . Including this result along with other recent mass measurements in the mixing angle prediction of Eq. (1) gives $\phi_P = (41.461 \pm 0.008)^\circ$.

We gratefully acknowledge the effort of the CESR staff in providing us with excellent luminosity and running conditions. This work was supported by the A.P. Sloan Foundation, the National Science Foundation, the U.S. Department of Energy, the Natural Sciences and Engineering Research Council of Canada, and the U.K. Science and Technology Facilities Council.

-
- [1] C. Amsler *et al.* (Particle Data Group), Phys. Lett. B **667**, 1 (2008).
- [2] J.L. Rosner, Phys. Rev. D **27**, 1101 (1983).
- [3] F.J. Gilman and R. Kauffman, Phys. Rev. D **36**, 2761 (1987), Erratum *ibid.* D **37**, 3348 (1988).
- [4] M. Ablikim *et al.* (BES Collab.), Phys. Rev. D **73**, 052008 (2006).
- [5] F. Ambrosino *et al.* (KLOE Collab.), Phys. Lett. B **648**, 267 (2007).
- [6] R. Escribano and J. Nadal, J. High Energy Phys. **05**, 006 (2007).
- [7] H.F. Jones and M.D. Scadron, Nucl. Phys **B155**, 409 (1979); H. Fritzsche and P. Minkowski, Nuovo Cim. **A30**, 393 (1975).
- [8] T. Feldmann and P. Kroll, Phys. Scripta **T99**, 13 (2002); T. Feldmann, P. Kroll, and B. Stech, Phys. Lett. B **449**, 339 (1999).
- [9] D. Kekez and D. Klabucar, Phys. Rev. D **73**, 036002 (2006).
- [10] J.-M. Gerard and E. Kou, Phys. Lett. B **616**, 85 (2005).
- [11] C. Michael, Phys. Scripta **T99**, 7 (2002).
- [12] H. Mendez *et al.* (CLEO Collab.), Phys. Rev. D **78**, 011102(R) (2008).
- [13] D.H. Miller *et al.* (CLEO Collab.), Phys. Rev. Lett. **99**, 122002 (2007).
- [14] Y. Kubota *et al.* (CLEO Collab.), Nucl. Instrum. Meth. A **320**, 66 (1992); M. Artuso *et al.*, Nucl. Instrum. Meth. A **554**, 147 (2005); D. Peterson *et al.*, Nucl. Instrum. Meth. A **478**, 142 (2002); CLEO-c/CESR-c Taskforces & CLEO-c Collab., Cornell University LEPP Report No. CLNS 01/1742 (2001), unpublished.
- [15] D.J. Lange, Nucl. Instrum. Methods Phys. Res., Sect. A **462**, 152 (2001).
- [16] R. Brun *et al.*, Geant 3.21, CERN Program Library Long Writeup W5013 (1993), unpublished.
- [17] J.G. Layter *et al.*, Phys. Rev. D **7**, 2565 (1973).
- [18] W.-M. Yao *et al.* (Particle Data Group), J. Phys. **G33**, 1 (2006) and 2007 partial update for 2008.
- [19] A. Duane *et al.*, Phys. Rev. Lett. **32**, 425 (1974).

TABLE I: For each decay mode, the number of events N , the Gaussian width on the mass distribution of those data events, σ , in MeV, the values of $\langle\delta\rangle$, β (from MC), and the difference $\langle\delta\rangle-\beta$ (see text), in keV. Uncertainties shown are statistical.

Mode	N	σ	$\langle\delta\rangle$	β	$\langle\delta\rangle-\beta$
A	2697	3.46	-71 ± 85	-61 ± 20	-10 ± 87
B	1017	1.93	-113 ± 69	-141 ± 13	28 ± 70
C	203	2.51	-9 ± 205	-54 ± 35	45 ± 208
D	230	1.95	-3 ± 147	-41 ± 19	38 ± 148

TABLE II: For each η' channel, systematic and statistical uncertainties in $M_{\eta'}$ (in keV) from the listed sources (see text); where applicable the degree of variation of the source level is given. The sources marked with a dagger (\dagger) are assumed to be fully correlated across all modes; others are assumed to be uncorrelated. The final column combines the uncertainties across all modes with the weights given in the text.

Source	Variation	A	B	C	All
Fit mass window		11	9	31	7
$M_{\psi(2S)}^\dagger$	34 keV	9	2	3	5
$M_{J/\psi}^\dagger$	11 keV	3	2	2	2
Bias	$(\beta_i + \Delta\beta_i)/3$	27	51	30	27
p_{π^\pm} scale	0.01%	28	17	25	15
E_γ scale	0.6%	13	22	28	12
M_η	24 keV		23		11
Systematic Sum		44	63	57	36
Statistical		87	70	208	54

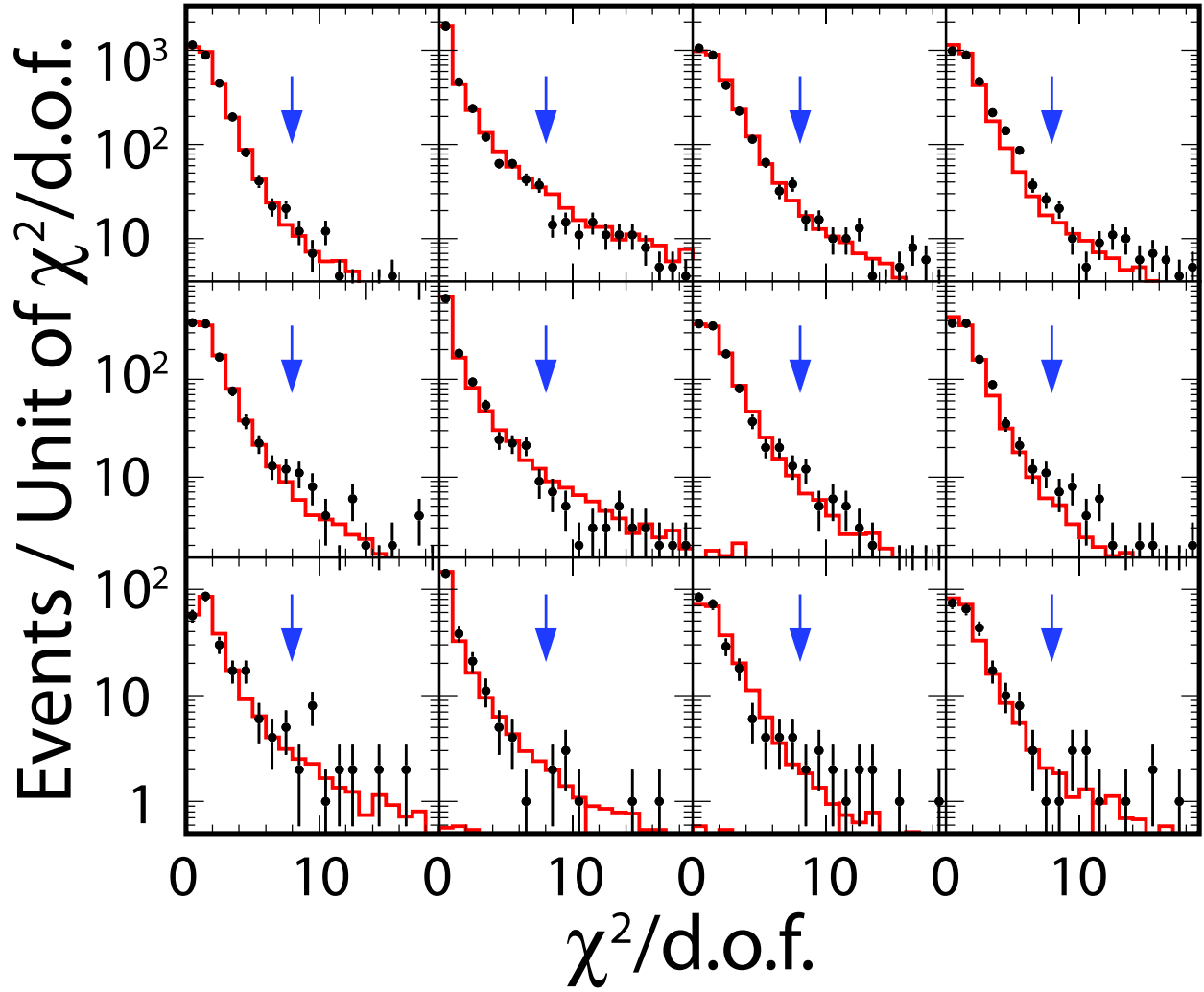


FIG. 1: Distributions of the fit quality for the kinematic constraint procedures described in the text, for, from top to bottom, modes A , B , and C , and, from left to right, J/ψ vertex fit, J/ψ mass fit, $\psi(2S)$ vertex fit, and $\psi(2S)$ four-momentum fit. Arrows indicate nominal selection criteria. The solid line histogram represents the signal MC prediction normalized to the number of events in the data.

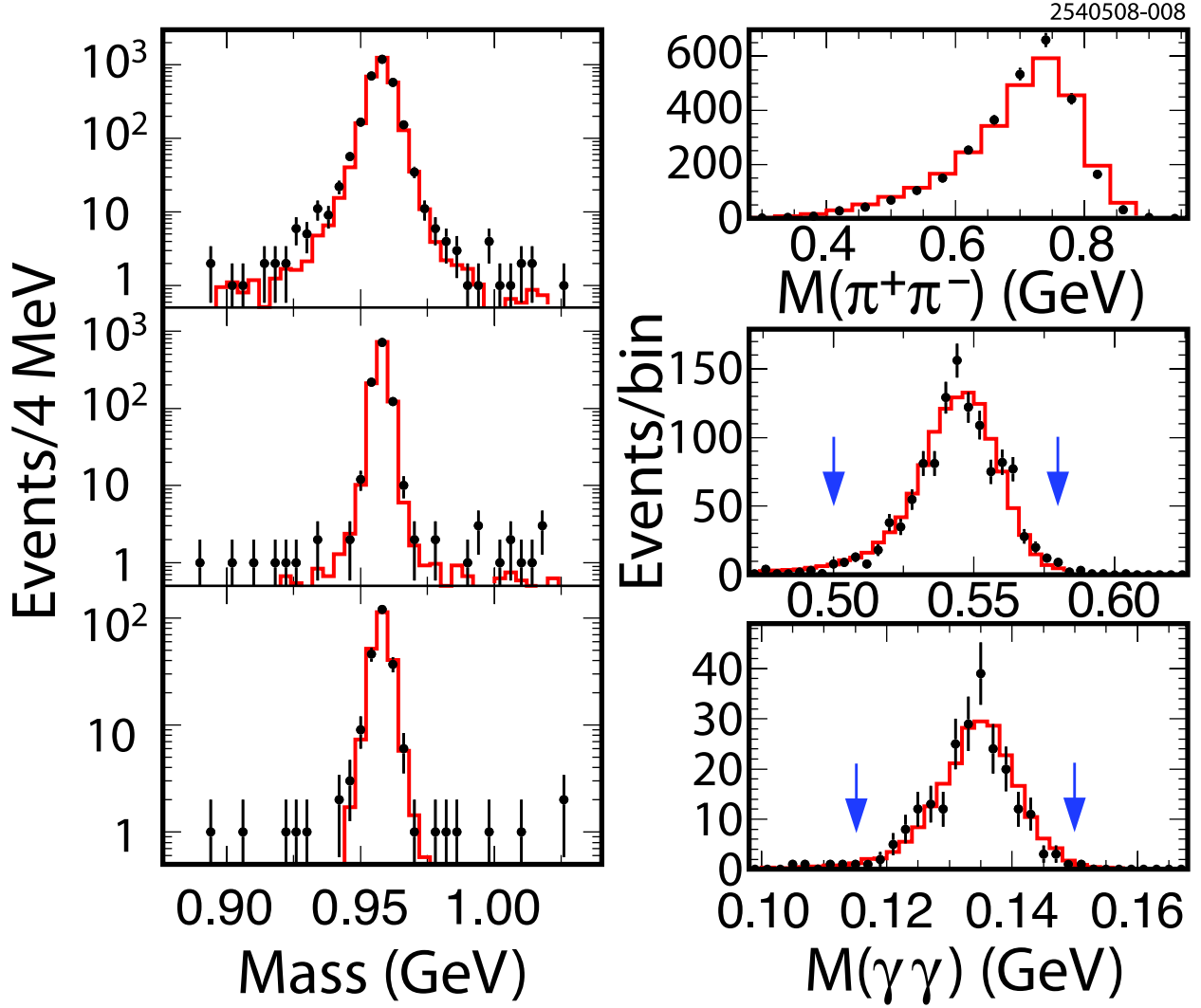


FIG. 2: Distributions of η' -candidate masses (left) for modes A (top), B (middle), and C (bottom). On the right, masses of intermediate particles: the $\rho^0 \rightarrow \pi^+\pi^-$ mass for mode A, the $\eta \rightarrow \gamma\gamma$ mass for mode B, and the $\pi^0 \rightarrow \gamma\gamma$ mass for mode C. Symbols are defined as in Fig. 1.

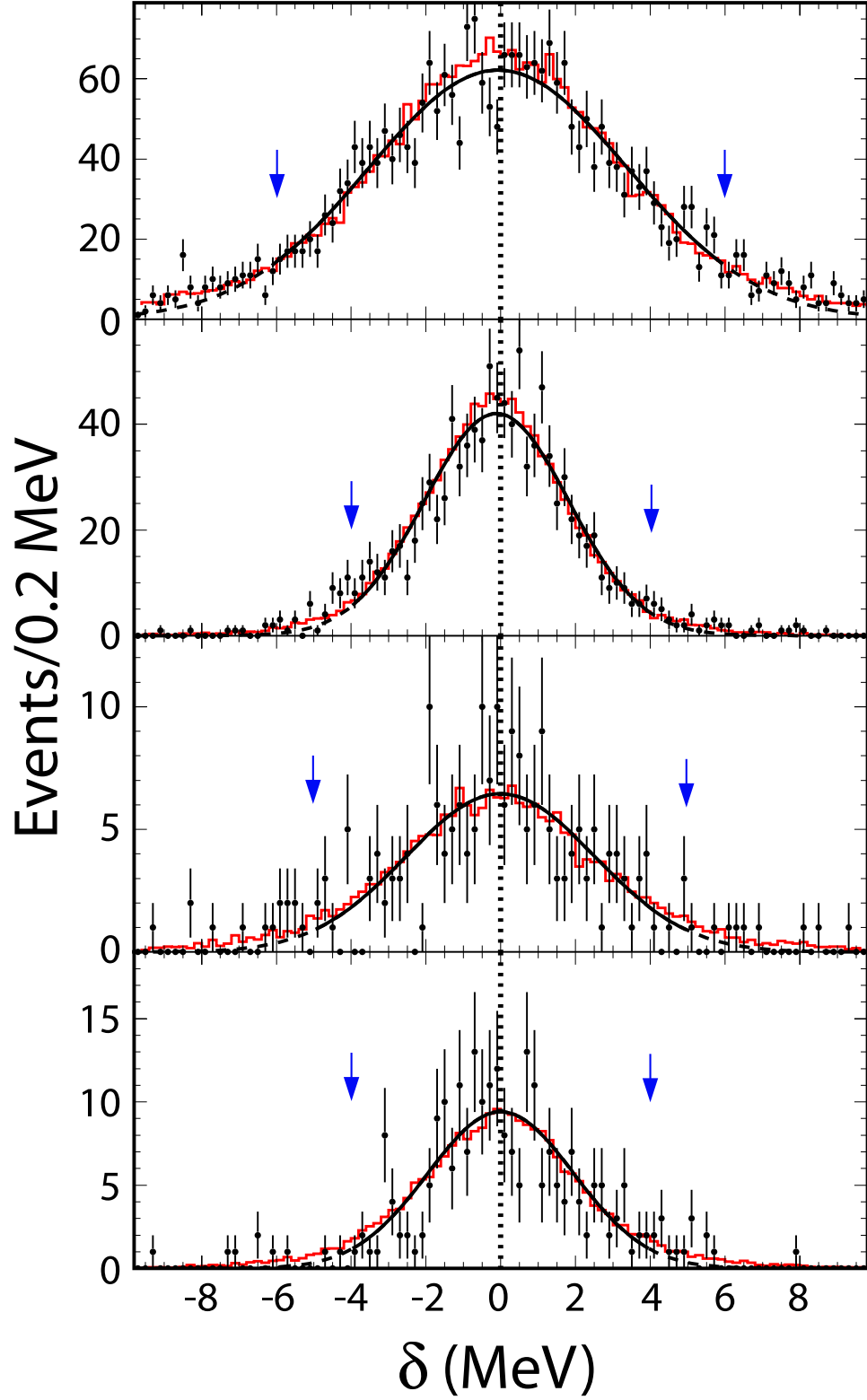


FIG. 3: Distributions of δ for, from top to bottom, modes *A*, *B*, *C*, and *D* (see text), with the data represented by the points with error bars and the Gaussian fit overlaid. The solid line portion of the Gaussian curve indicates the mass window used for the fit and the dashed portions its extension. The solid line histogram represents MC simulation of signal, normalized as in Figs. 1 and 2.